Signal processing from a detector of a radiometric density meter - results of empirical studies

Signal processing from a detector of a radiometric density meter - results of empirical studies

S Cierpisz[1], **J Joostberens**[2] **and W Sobierajski**[3]

[1] Institute of Innovative Technologies EMAG, 31 Leopolda, 40-189 Katowice, Poland
[2] Silesian University of Technology, Faculty of Mining and Geology, 2 Akademicka Street, 44-100 Gliwice, Poland
[3] Institute of Innovative Technologies EMAG, 31 Leopolda, 40-189 Katowice, Poland

E-mail: jaroslaw.joostberens@polsl.pl

Abstract. The paper presents the results of signal processing from an industrial radiometric density meter with a ^{137}Cs gamma radiation source and a scintillation counter as a detector. There are presented the results of the most important stages of signal processing from the detector, such as the formation of the pulse series to the digital form, counting pulses by the meter and determining the density values based on the calibration characteristics of the device. The principles of density meter calibration were also presented in the case of using the whole ^{137}Cs radioactivity spectrum as well as for the photopeak. The probability distributions of the impulse series from the detector before and after the isolation of the photoeak were presented and compared with the theoretical Poisson distribution. The measurement time is an essential parameter determining the dynamic properties of the density meter. The paper presents an example of empirical selection of measurement time in case of step density change.

1. Introduction

Radiometric density meters are widely used for monitoring and control of various technological processes, including hard coal preparation in processes such as: separation in heavy media, separation in jigs and coal flotation. They operate on the principle of absorption of gamma radiation passing through a layer of material (absorbent). The intensity of radiation after passing through the absorbent describes the equation:

$$I(t) = I_0 \cdot e^{-\mu_d \cdot d \cdot \rho(t)} \tag{1}$$

- I_0 – gamma radiation intensity without absorbent,
- μ_d – attenuation coefficient,
- d – absorbent thickness,
- ρ – density of the absorbing layer.

The radiometric density meter consists of two main components: a measuring head and an electronic system. The measuring head consists of a gamma ray source (^{137}Cs) and a radiation detector - usually a scintillation counter. The pulse series at the detector output is a stochastic signal with the Poisson distribution and the intensity λ, which is a measure of the monitored density:

$$P(k) = \lambda^k \cdot e^{-\lambda} \cdot (k!)^{-1} \tag{2}$$

- $P(k)$ – the probability of counting k of impulses during the time of measurement t_s.

The signal from the detector is sent to the input of the pulse counter, which counts the pulses within a certain time interval called the measurement time t_s, as shown in figure 1.

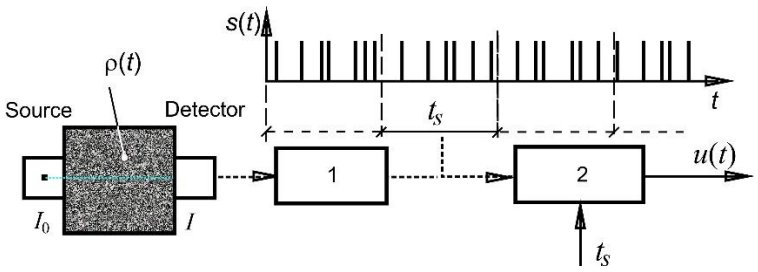

Figure 1. Processing the signal from the detector using the pulse counter.
1 – electronic processing system, 2 – counter

The number of pulses counted during the measurement is converted into the measured signal on the basis of the empirical relation between the density and the mean number of pulse counts per second. The dynamic properties and the accuracy of the density meter depend mainly on the measurement time t_s. The issue of selecting the time of measurement of the density meters used in the monitoring systems of the coal separation process in the jig was discussed in [1] [2]. As reported in [2], the application of an additional low-pass filter at the output of the meter may improve its dynamic properties without influencing its static accuracy. The method of signal processing in an industrial radiometric density meter is presented on the example of empirical measurements of pulse series under various conditions of the radiation beam attenuation. Optimal measurement time was also determined for the step change in density when using the entire radiation spectrum as well as the photopeak only.

2. Laboratory measurements

2.1. Laboratory stand

Laboratory tests were carried out on the test stand shown in figure 2.

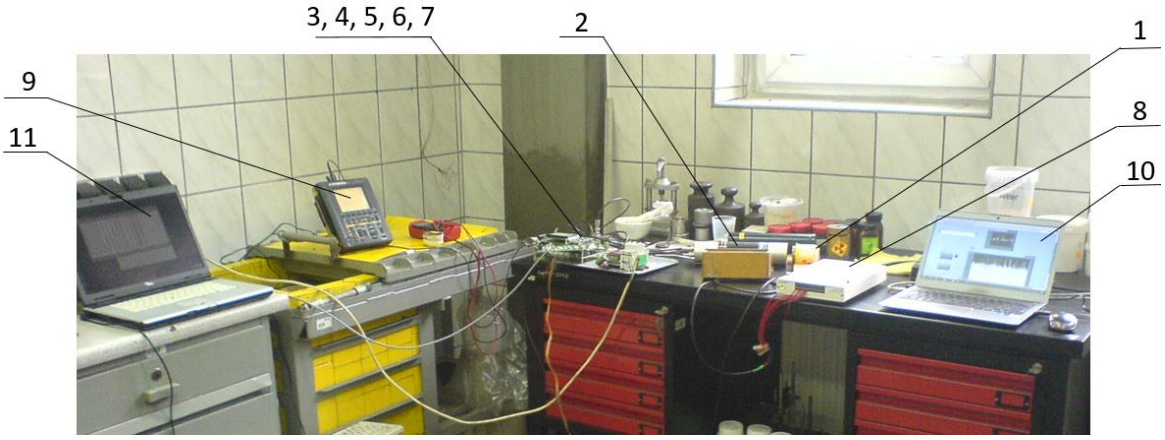

Figure 2. Laboratory stand for testing the radiometric density meter.

The way of connection of the measuring devices (points $p1$ and $p2$) is shown in the schematic diagram (figure 3).

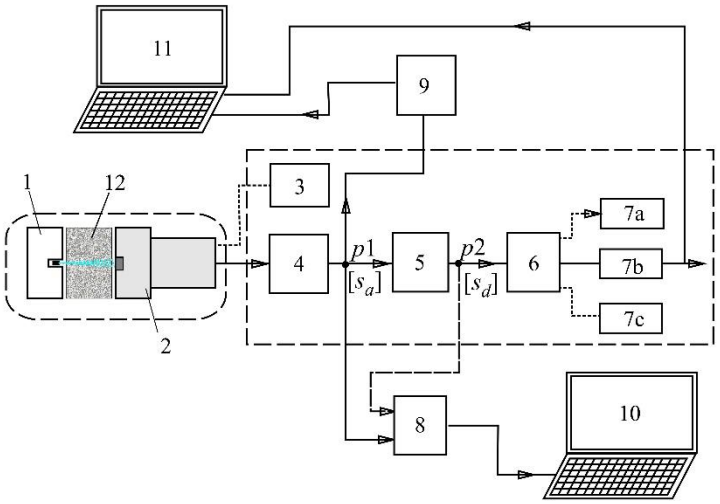

Figure 3. Schematic diagram of the system for testing the radiometric density meter.

The basic elements of the laboratory stand are (figures 2 and 3):

- radiation source (1),
- detector (2),
- high-voltage power supply (3),
- a signal amplifier system from a detector with a multi-channel spectrum analyzer (4),
- pulse forming system for the 0-5V digital standard (the photopeak range of the radiation spectrum) (5),
- pulse counter (6),
- transmission block (7a) with display (7b) and I/O block (7c),
- recording system based on NI USB-6259 with 32-channel analogue input card (8),
- oscilloscope (9),
- a PC computer with LabVIEW software (10),
- a PC for recording the number of pulses counted by the electronic counter (11).

As a source of gamma radiation, a ^{137}Cs isotope was used, due to its widespread use in industrial radiometric density meters [3, 4, 5]. A scintillation counter (2) of the ENGELHARD 6SHAB/2A type (figure 2) with NaI(Tl) crystal was used to detect radiation. In the radiometric meter, the counting function for the measurement time t_s is carried out by an electronic counter (6), reacting to the rising edge of the 5V digital signal. The basic analysis of empirical data was made on the basis of measurements made with the units (8) and (9) connected in points $p1$, $p2$ - figure 3. The selection of the sampling frequency was determined by the duration of a single pulse.

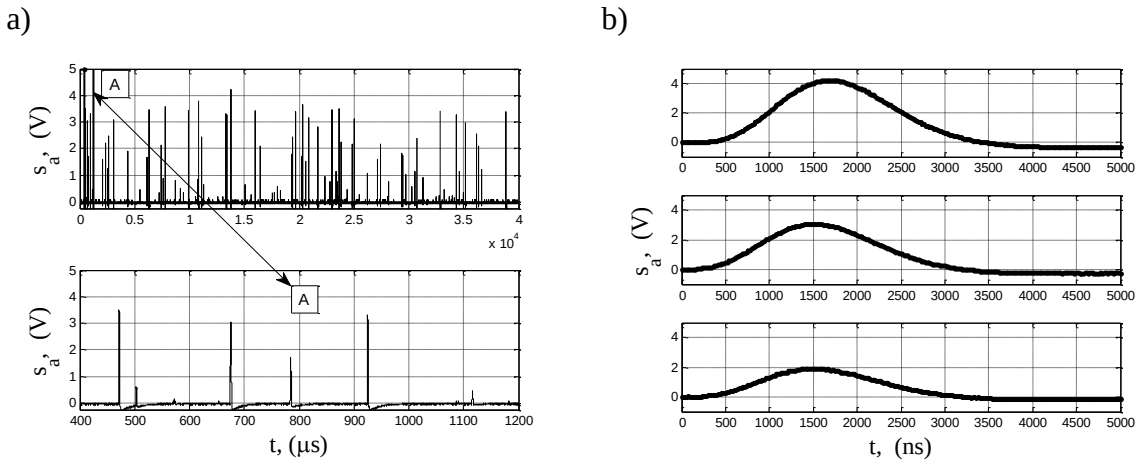

Figure 4. Example of registered pulses from a radiation detector (point *p*1). a) pulse series, b) pulses with different peak values

The pulse duration was measured using a NI USB-5133 oscilloscope, with a sampling rate of 50MS/s. Sample waveforms of recorded pulses with various peak values are shown in figures 4a, b. The results of the measurements showed that the time of a single pulse is longer than 2μs, and the time between successive pulses many times exceeds 1μs. Therefore, signal sampling at 1MS/s to detect the occurrence of pulses was considered sufficient. Due to the faster rise of the slope, the recording of the impulse series after their digitization s_d (point *p*2) was carried out at the frequency of 1.25MS/s. For registration and observation in a discrete way, the National Instruments NI USB-6259 recording system was used. Impulse signals in the form of an analogue signal before their digitalization (point *p*1 in figure 3), as well as after their processing into rectangular pulses were registered. One of the 32 available analogue inputs of this system was used, thus ensuring a sufficiently high sampling frequency. In order to ensure data registration, software was developed in the LabVIEW environment, enabling the observation of the pulse time course and lossless data storage to a computer disk (10). The program was developed in G language based on the "*producer - consumer*" architecture to ensure reliable registration of all data at such a high sampling rate.

2.2. Test conditions

The tests included recording of a pulse series in the situation of:

- no absorbent - only atmospheric air (reference measurement) occurs between the radiation source and the detector,
- placing absorbents in the space between the source and the detector.

In the first stage of the research, signal waveforms s_a (point *p*1) were recorded in the range of the whole spectrum of the radiation source, and then the signal s_d (point *p*2) in the range of the ^{137}Cs spectrum photopeaks. Absorbers with a surface density of $\rho_{a1} = 4.2$ and $\rho_{a2} = 5.9$ g·cm^{-2} were used. The results of the tests are presented in tables 1 and 2. Additional symbols were adopted: ρ_0 - air density, ρ_{a3} - density resulting from the use of both absorbents simultaneously. Measurements were made in 5-second time periods, so a data series was obtained with a number of samples no less than 5,000,000. A background radiation was measured each time before the actual tests were started. The developed program working in the Matlab software performed digital processing of empirical data according to the following algorithm:

- reading of measurement data,
- processing of the data string to the 0-5V digital standard, (in the case of a (the) s_a signal),

- processing a 0-5V digital signal into a unit pulse series,
- adding pulses in subsequent time intervals, corresponding to the measurement time t_s.

Figure 5 presents the results of software operation that implements the above algorithm for an exemplary time interval of about 125 μs.

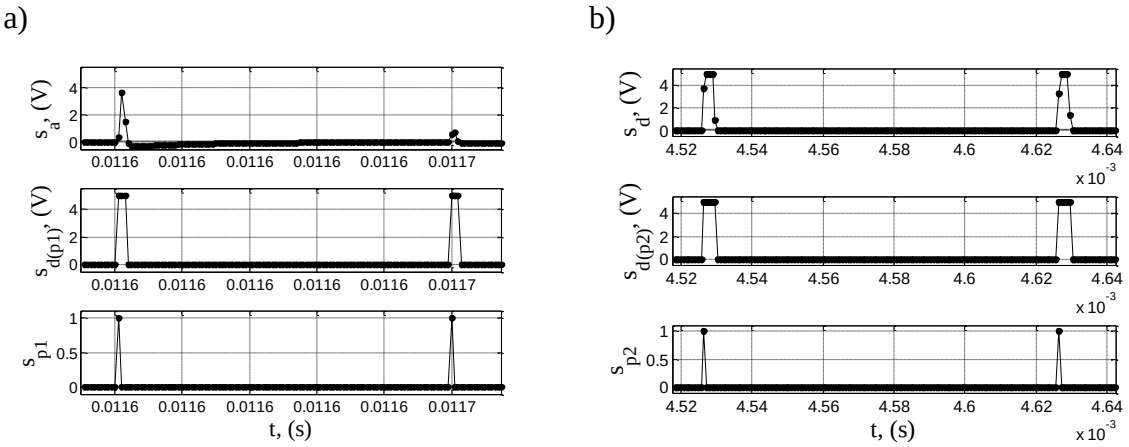

Figure 5. Sample results of software processing of registered signals measured in points a) $p1$ and b) $p2$.

As it can be seen in figure 5a, the registered analog signal (s_a) from the radiation detector (after amplification) contains pulses with various amplitude values, less than 5V. The signal [s_a] is programmed into a sequence of rectangular pulses of different duration [$s_{d(p1)}$], but with the same amplitude values (5V). In the case of the signal measured in point $p2$ (figure 5b), the pulses have peaks of about 5V and a rectangular shape. Signals with rectangular pulses $s_{d(p1)}$ and $s_{d(p2)}$ are processed into the unit pulse series (s_{p1}, s_{p2}), as shown in figures 5a, b. The appearance of a single pulse occurs when the slope of the rectangular pulse increases. A "unit impulse" is a normalized pulse with an amplitude value at the time of its appearance equal to one, and for the remaining moments - zero [6]. The data sequences prepared in this way were used to count pulses at any time intervals corresponding to the measurement times. This operation imitate the work of the electronic pulse counter. Impulse counts were performed for all data series, using the following measurement times: 5ms, 10ms, 20ms, 25ms, 50ms and an additional 0.5s and 1s. Strings of the counted pulses for the adopted measurement times were used to determine the probability distributions to check their compliance with the theoretical Poisson distribution described by equation (2). Evaluation of measurement results in statistical terms requires checking whether k can be treated as a random variable with Poisson distribution with parameter λ. Probability distributions for empirical data were made for several measurement times.

3. Results of laboratory tests

The measurements were preceded by the determination of the mean number of pulse counts from the background radiation. It was found that this value did not exceed 5% of the number of counts without absorbent. Using the multichannel spectral analyzer, spectra were determined for various materials between the source and the detector (air, absorbents). Exemplary spectra of the radiation source used are shown in figure 6, where channels correspond to the energy of gamma photons in keV.

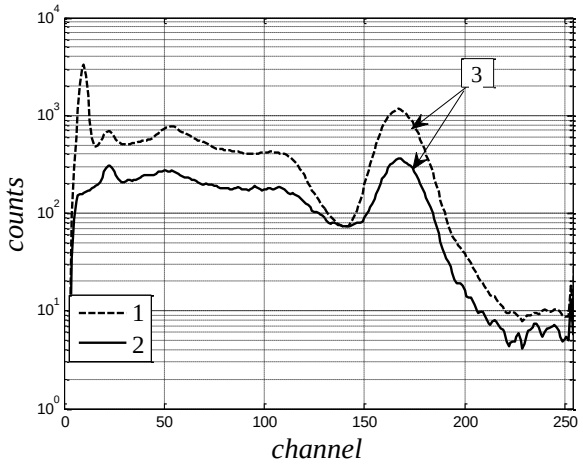

Figure 6. ^{137}Cs gamma ray spectrum recorded using a scintillation counter. 1 – no absorbent, 2 – absorbent with density ρ_{a3}, 3 - photopeaks

The recorded data series were used to determine the probability distributions for various absorbers and measurement times. This was connected with the determination of the number of pulses *k* per time unit, i.e. with the summation of pulses in intervals on the time axis corresponding to the measurement times. Exemplary results of pulse counting in the period of 0.5 s for two different measurement times are shown in figure 7. The results of the tests are presented in tables 1 and 2, figures 8 and 9. The values of the mean number of counts and variance (D_y) are approximated to the integer.

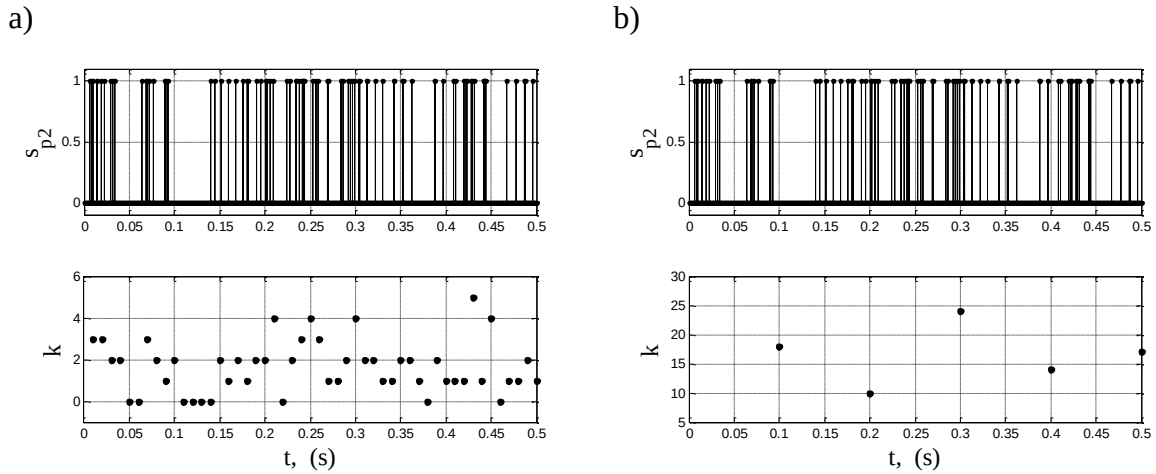

Figure 7. Part of the pulse series and result of counts in the case of using an absorbent with density ρ_{a3} for two measurement times a) 10 ms and b) 100 ms (table 2).

It should be noted that the research results in the form of empirical distributions show convergence with the theoretical distribution in each of the considered cases, i.e. in the situation of different materials between the source and the detector (air, absorbents), as well as different measurement times t_s. Examples of empirical and theoretical distributions are shown in figures 8 and 9. Significant convergence of empirical distributions with the Poisson theoretical distribution is also confirmed by the results of the calculated mean values of the number of pulses (λ) at the time of t_s and variance. As can be seen in tables 1 and 2, the equality (approximately) between the determined mean number of counts and the variance occurs in each case, regardless of the measurement time used. Therefore, *k* can be

treated as a random variable with the Poisson distribution with the parameter λ. In addition, there was a significant convergence between the results of counts per second obtained on the basis of registered data series, with electronic counter counts. This indicates the correct operation of the monitoring system and the signal processing algorithm used.

Table 1. The results of statistical analysis of signals from the radiation detector for the entire spectrum of the radiation source.

t_s (ms)	ρ_0 (g cm^{-3})		ρ_{a1} (g cm^{-3})		ρ_{a2} (g cm^{-3})		ρ_{a3} (g cm^{-3})	
	0.0013		3.41		4.78		8.13	
	λ	D_y	λ	D_y	λ	D_y	λ	D_y
5	11	11	6	6	6	6	4	4
10	22	21	12	12	11	13	7	8
20	43	44	24	23	23	27	15	16
25	54	56	30	31	28	34	18	18
50	109	109	60	52	57	68	36	37
100	217	179	119	81	114	126	73	85
500	1087	-	598	-	569	-	367	-
1000	2174	-	1196	-	1138	-	733	-

Table 2. The results of statistical analysis of signals from the radiation detector for the photopeak of the radiation source

t_s (ms)	ρ_0 (g cm^{-3})		ρ_{a1} (g cm^{-3})		ρ_{a2} (g cm^{-3})		ρ_{a3} (g cm^{-3})	
	0.0013		3.41		4.78		8.13	
	λ	D_y	λ	D_y	λ	D_y	λ	D_y
5	3	3	2	2	2	2	1	1
10	6	6	4	4	3	3	2	2
20	11	13	8	8	6	5	4	4
25	14	16	10	12	8	7	5	5
50	28	35	19	21	15	15	9	11
100	55	68	38	49	30	35	19	20
500	275	-	192	-	152	-	94	-
1000	551	-	383	-	303	-	187	-

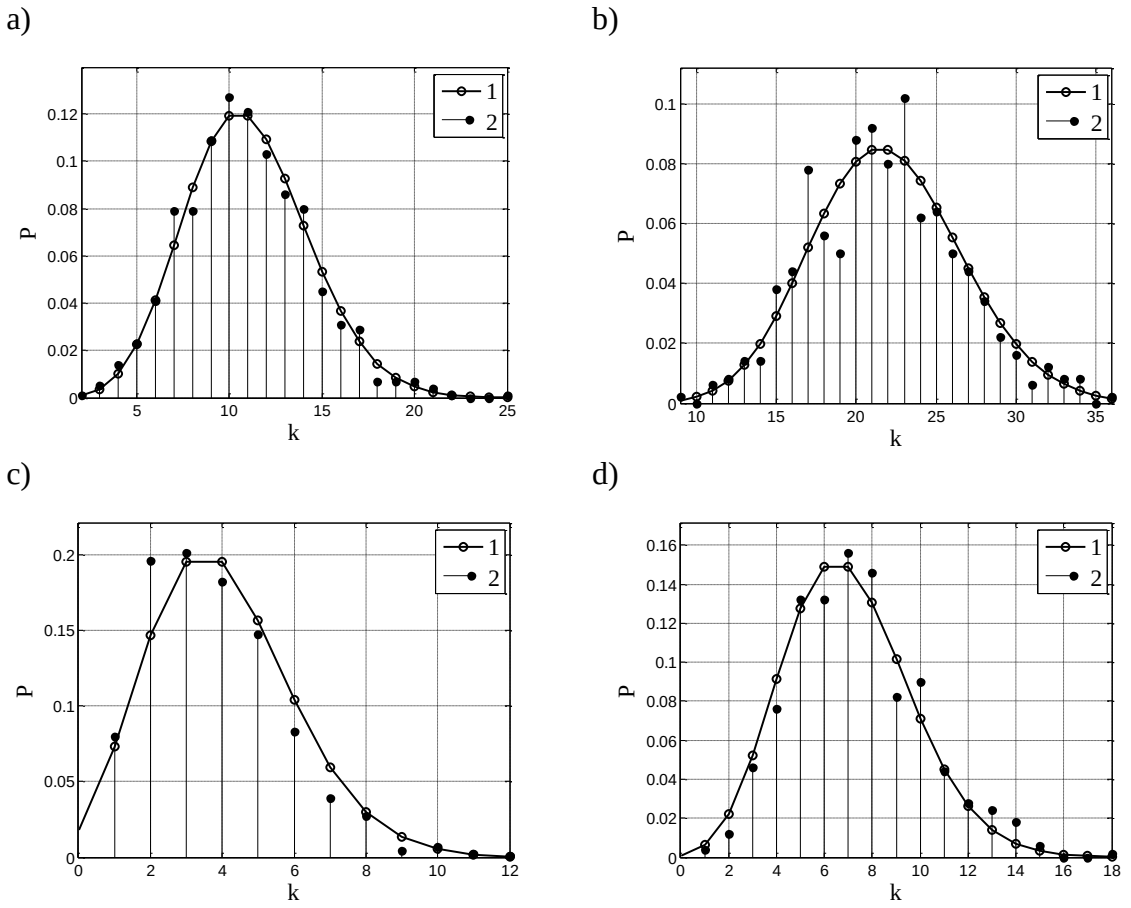

Figure 8. Empirical (2) and theoretical (1) Poisson distributions for the cases given in Table 1 (ρ_0 and ρ_{a3}) for two measurement times equal to a), c) 5 ms and b), d) 10 ms

The values of the mean number of counts λ from tables 1 and 2 for the measurement time equal to 1 s were used to determine the empirical relation between the counts rate and the density. This operation is equivalent to determining the calibration characteristics of an industrial radiometric density meter. By converting equation (1) as follows

$$\rho = -(\mu \cdot d)^{-1} \cdot \ln(I \cdot I_0^{-1}) = -(\mu \cdot d)^{-1} \cdot \ln(k_1 \cdot \lambda_0^{-1}) \tag{3}$$

and taking into account that the average number of pulses per 1 second λ_0, registered during measurements without absorbent, is a reference, we can write

$$\rho = \ln(\lambda_0) \cdot (\mu \cdot d)^{-1} - \ln(k_1) \cdot (\mu \cdot d)^{-1} = a_0 - a_1 \cdot \ln(k_1) \tag{4}$$

- k_1 – number of pulses counted for the measurement time t_s and standardized to 1 s,
- a_0, a_1 – parameters of the calibration characteristics.

In this situation, the identification task comes down to determining the model parameters (4). In practice, the dependence (4) can be replaced by the linear equation of the form:

$$\rho = b_0 - b_1 \cdot k_1 \tag{5}$$

Then b_0, b_1 are the parameters of equation (5), and this relationship applies to density changes in the range [ρ_{a1}, ρ_{a3}]. To determine the parameters of equations (4) and (5), the least-squares method was used, and the coefficient of determination R^2 was used as a criterion for fitting the model to the empirical data.

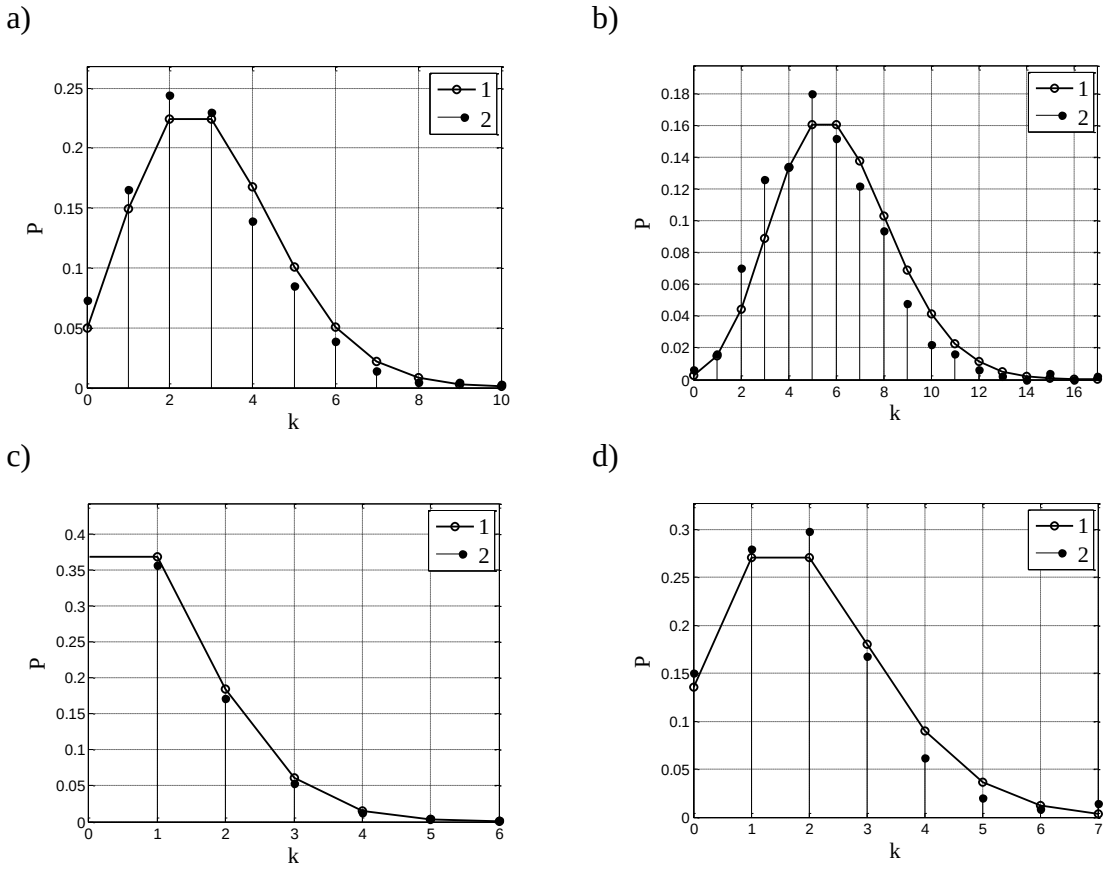

Figure 9. Empirical (2) and theoretical (1) Poisson distribution for the cases given in table 2 (ρ_0 and ρ_{a3}) for two measurement times equal to a), c) 5 ms and b), d) 10 ms

Table 3. Results of the approximation of the calibration characteristics of the radiometric density meter.

Figure	a_0	a_1	R^2	b_0	b_1	R^2
10a	56.784	7.428	0.978	15.378	0.010	0.988
10b	47.028	7.403	0.991	12.553	0.024	0.983

The approximation was carried out for two data series - obtained for the entire gamma-ray spectrum (table 1) and for the spectral range corresponding to the photopeak (table 2). The results of the approximation of the dependence $\rho = f(k_1)$ are presented in table 3 and are shown in figure 10. It should be noted that the mathematical models (4) (5) show a good fit to the empirical data.

a) b)

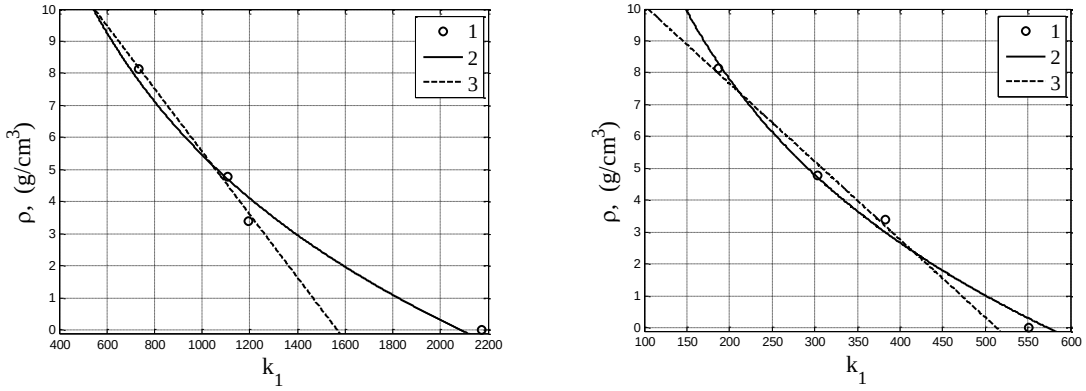

Figure 10. The calibration characteristics of the radiometric density meter in the situation of a) the use of the entire ^{137}Cs radiation spectrum and b) the spectral range of the photopeak.
1 – measurement data, 2 – model with equation (4), 3 – model with equation (5) for the range [ρ_{a1}, ρ_{a3}]

4. Selection of measurement time

The signal processing from the gamma radiation detector in industrial radiometric density meters is of a multi-stage nature. The last stage is the counting of pulses with a properly selected time of measurement t_s, or with an additional digital low-pass filter mounted on the meter output. The selection of the measurement time mainly determines the dynamic properties of the radiometric meter. In the case of a constant density of the medium (ρ = const), the measurement signal contains a Poisson noise which produces an error in determining the calibration characteristics. This error is lower for the longer measurement time. On the other hand, the long measuring time increases the dynamic measurement error due to the increased inertia of the monitoring system. The radiometric density meter, used to control the coal separation process, should have the measurement time t_s chosen so as to ensure a significant reduction of noise in the output signal without deteriorating its dynamic properties. The choice of the optimal value of time t_s, and thus the selection of the filter parameter, can be carried out for a given density change in time. In this case, the mean squared error is defined as:

$$MSE_j = N^{-1} \cdot \sum_{i=1}^{N} \left(u_j[i] - \rho[i]\right)^2 \tag{6}$$

- N_1 – the number of data used to determine the parameter t_s,
- u_j – the value of the signal from the density meter in the moment $t = i \cdot \Delta t$ determined on the basis of pulse counts during the period of time t_s using the equation j (4 lub 5)
- ρ – the density signal step change from the value of ρ_{a1} to ρ_{a3} at the time of 2.5s

MSE_j is an error calculated for the selected implementation of the measurement run. As part of empiric studies, the sequence of impulses from the detector was recorded in points $p1$ and $p2$, as a response to the step change in density from the value of ρ_{a1} to the value of ρ_{a3}, obtained by quickly placing the absorbent. The parameter t_s was chosen to minimize the value of criterion (6) for the considered time interval, using the same sampling period Δt = 1 ms for all obtained signals**.** The step change in density over time was assumed as a reference signal (figure 11). The results of the tests are presented in the table 4 and figures 11a, b. These results relate to one run of registered stochastic signals and are not a generalization of the problem.

Table 4. The results of an exemplary selection of the measurement time.

Equation	Point $p1$		Point $p2$	
	t_s (ms)	*MSE*	t_s (ms)	*MSE*
4	170	0.9342	210	1.3507
5		0.8198		1.2439

As it can be seen in figure 11, signals from the density meter show a significant convergence with the reference signal (density). This shows that the selected measurement times ensure good attenuation of the fast-changing noise in the output signal without a significant deterioration of the dynamic properties of the density meter. Better matching of empirical data to the reference density change occurs using the full ^{137}Cs source spectrum. The choice of the calibration characteristics in the form of one of the equations (4) (5) in the considered range of density changes has no significant effect on the results. This shows that a linear calibration characteristic can be used for a small range of density changes.

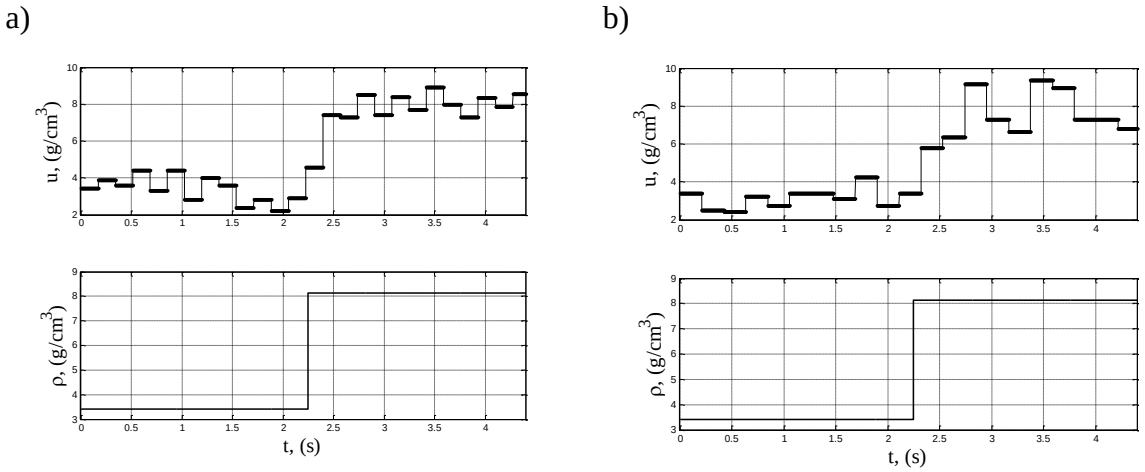

Figure 11. Signals $u(t)$ for selected measurement times t_s determined on the basis of signals measured in points a) $p1$ and b) $p2$, as a responses to the step change in the density ρ.

5. Conclusions

Laboratory tests of the radiometric density meter enabled the analysis of the real measurement signal from the radiation detector. The detector was a scintillation counter. The simplest low-pass filter in the form of a pulse counter with the measurement time t_s was used. All tests were conducted for the entire radiation spectrum and the photopeak itself. The analysis of the measurement data showed a good convergence of probability distributions with the theoretical Poisson distribution. Equality (numerical) of the empirical average value of pulse rate with signal variance was confirmed, which is a characteristic feature of the Poisson distribution.

It has been shown that for the practical range of changes in the measured density, the calibration characteristics resulting from the exponential absorption law can be approximated with a linear relationship with good accuracy.

The simplest filter of the radiation detector's signal is the pulse counter with the selected measurement time. For a short measurement time, the statistical measurement error is large, and the dynamic error is small, which results from the meter's rapid response to the changing number of pulses. For a long measurement time, the statistical error is small because the noise of the stochastic component is better filtered and the dynamic error is large. There is therefore an optimal measurement time for

which the mean square error is the smallest. The value of this time depends on the shape of changes in the density measured as a function of time. The total measurement error, resulting from the dynamic properties of the meter and the stochastic nature of the pulse series from the detector, is the smaller the higher is the mean number of pulses from the detector. Hence, a smaller measurement error can be obtained. in the same measurement conditions, for the entire radiation spectrum than for the photopeak. This conclusion does not take into account additional measurement errors resulting from the influence of changes in the chemical composition (changes in the attenuation coefficient) of the absorbent.

6. References

[1] Cierpisz S and Joostberens J 2016 *Measurement*, **88** 147
[2] Cierpisz S and Joostberens J 2016 *17th IFAC Symposium on Control, Optimization and Automation in Mining, Mineral and Metal Processing (Vienna)* p 45
[3] Astafieva I M, Gerasimov D N and Makseev R E 2017 *J. Phys.: Conf. Ser.* **891** 012322
[4] Będkowski Z, Kot D, Krodkiewski J, Mironowicz W and Sikora T 2008 *21st World Mining Congress & Expo (Katowice)* p 49
[5] Clarkson C, Hornsby D and Walker D 1993 *Coal Preparation* **12** 41
[6] Smith S W 2002 *Digital Signal Processing: A Practical Guide for Engineers and Scientists* (Elsevier)

Acknowledgments

Acknowledgement goes to the Institute of Innovative Technologies EMAG for providing the laboratory test stand.